



**HAL**  
open science

## Implementation of a VHF Spherical Near-Field Measurement Facility at CNES

Gwenn Le Fur, Guillaume Robin, Nicolas Adnet, Luc Duchesne, Daniel Belot,  
Lise Feat, Kevin Elis, Anthony Bellion, Romain Contreres

► **To cite this version:**

Gwenn Le Fur, Guillaume Robin, Nicolas Adnet, Luc Duchesne, Daniel Belot, et al.. Implementation of a VHF Spherical Near-Field Measurement Facility at CNES. AMTA 2016, Oct 2016, Austin, United States. hal-01523536

**HAL Id: hal-01523536**

**<https://hal.science/hal-01523536>**

Submitted on 16 May 2017

**HAL** is a multi-disciplinary open access archive for the deposit and dissemination of scientific research documents, whether they are published or not. The documents may come from teaching and research institutions in France or abroad, or from public or private research centers.

L'archive ouverte pluridisciplinaire **HAL**, est destinée au dépôt et à la diffusion de documents scientifiques de niveau recherche, publiés ou non, émanant des établissements d'enseignement et de recherche français ou étrangers, des laboratoires publics ou privés.



Distributed under a Creative Commons Attribution 4.0 International License

# Implementation of a VHF Spherical Near-Field Measurement Facility at CNES

Gwenn Le Fur, Guillaume Robin,  
Nicolas Adnet, Luc Duchesne  
R&D Department  
MVG Industries  
Villebon-sur-Yvette, France  
Gwenn.le-fur@satimo.fr

Daniel Belot, Lise Feat, Kevin Elis,  
Anthony Bellion, Romain Contreres  
DCT/RF/AN  
CNES  
Toulouse, France  
Daniel.belot@cnes.fr

**Abstract**—This paper presents last implementation of a complete near-field system including probe positioner upgrades to reach positioning repeatability and ergonomy, an optical alignment tool, a specific reference antenna and a post-processing tool.

## I. INTRODUCTION

Needs of antenna measurements at low VHF range imply the development of specific facilities. Costs saving could be found by reusing existing chambers and extending the frequency band down to a few tens of MHz, especially if the implementation of such a system is performed in undersized chambers with already existing absorber materials. CNES began such an adaptation in the 2000's by adding a VHF measurement probe (80-400 MHz) in their CATR chamber which allows performing spherical near-field measurement. In the past four years, intensive studies have been conducted to reduce measurement results uncertainties and extend again the lower frequency down to 50 MHz. Major error terms were identified [1] and both new measurement probe and post processing tools have been already designed and implemented. This paper aims to present the hardware and software upgrades. Details are first provided on the mechanical upgrade of the probe positioner aiming to improve the positioning accuracy and repeatability as well as the ergonomy to save installation time. A reference antenna in gain and polarization has been specially developed, manufactured and validated. Such reliable reference antennas at these frequencies are a key point. Finally, optical tool for aiding the alignment of the measurement probe and the Antenna Under Test (AUT) as well as the post processing tool complete the system in order to master measurement uncertainties.

## II. CNES VHF NEAR-FIELD FACILITY

The system used is the single probe spherical near field system located in the chamber of the CNES in Toulouse France. This facility was dedicated to perform antenna measurement from 80 MHz to 200 GHz. The chamber is shared by a compact range measurement system and the considered single probe near-field system. Above 400 MHz the compact range configuration is used. Below 400 MHz the near-field configuration is used. Such cohabitation is possible thanks to the AUT positioner allowing spherical movement and to the removable near-field probe positioner. Nevertheless classical

foam pyramidal absorbers are poorly efficient below 200 MHz. Therefore ripples due to reflections coming from the compact range reflector and from the chamber walls are present and need to be bear in mind and taken into account while examining the measured data. In order to extend the operational measurement bandwidth down to 50 MHz a new wide band and dual polarized VHF probe has been designed and manufactured [1] (cf. Figure 1. ).

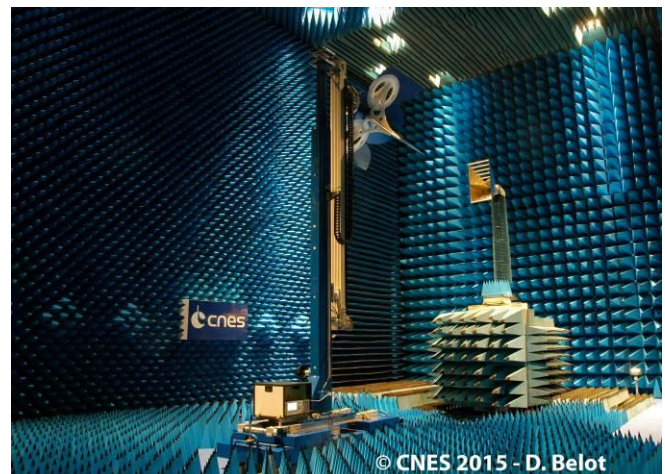


Figure 1. Photograph of the CNES VHF Near-Field system with the dual polarized probe

Conducted studies have allowed hardware upgrades and additions as well as alignment and post-processing tools. All of these led up to a comprehensive updated near-field system whose the main features are summarized herein after and described in this paper.

- The upgraded probe positioner with ergonomic and tuning axes
- The specified location of the probe positioner inside the chamber with positioning repeatability thanks to the anchor points. As the near-field probe is removed when performing far-field measurement using CATR configuration the relocation of the probe positioner had to be ensured

- The scan configuration to cover the full sphere around the AUT [2].  $\Phi$  scan [3] is used as shown in Figure 2.
- The optical alignment tool to relocate the probe in the nominal location
- The wide-band and dual polarized measurement probe
- The reference antenna dedicated to the calibration of the measurement probe in polarization and gain
- The post-processing tool including near-field to far-field transformation and time filtering to mitigate reflections impact coming from the chamber

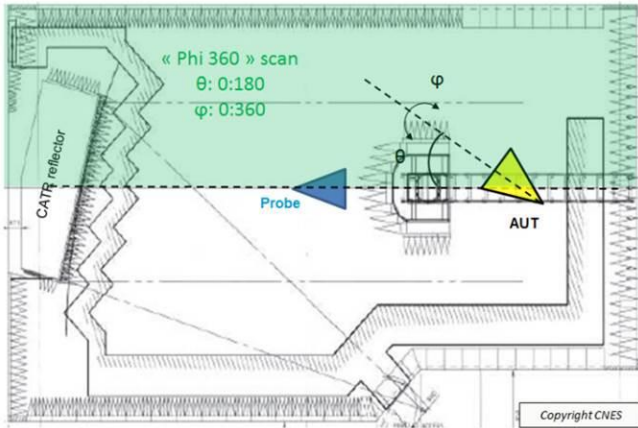


Figure 2. Layout of the near-field probe and the AUT in the CNES CATR chamber

### III. PROBE POSITIONER UPGRADE

A general overview of the updated probe positioner is given in Figure 3. The update consisted in adding ergonomic and positioning features to the existing material. To save costs and keep ease of use, no motorization was added – all axes are moved manually. Concerning probe positioning features, the following degrees of freedom were developed and integrated:

- Three pistons supporting the base frame in order to adjust its plane
- A Z-sliding axis on the base frame allowing to adjust the measurement distance
- A Y-sliding axis on the vertical mast allowing to adjust the height of the probe on the measurement axis
- A Roll axis behind the probe flange allowing to adjust the  $\pm 45^\circ$  orientation of the two probe polarizations

All these axes are used with the optical alignment tool described in the next part. As mentioned above the probe positioner is removable thus the base frame includes wheels. Nevertheless to ensure positioning repeatability of the base frame three anchor hemispheres were added to this frame (cf. Figure 4. ). To fit with, corresponding containers were fixed into the chamber floor (cf. Figure 5. ). This part is detailed hereafter and then the ergonomic aspects.

During installation campaign the whole positioner has been optically characterized by using laser tracker instrument. The

chosen location and axes adjustments take into account the positioner deformation in the measurement configuration.

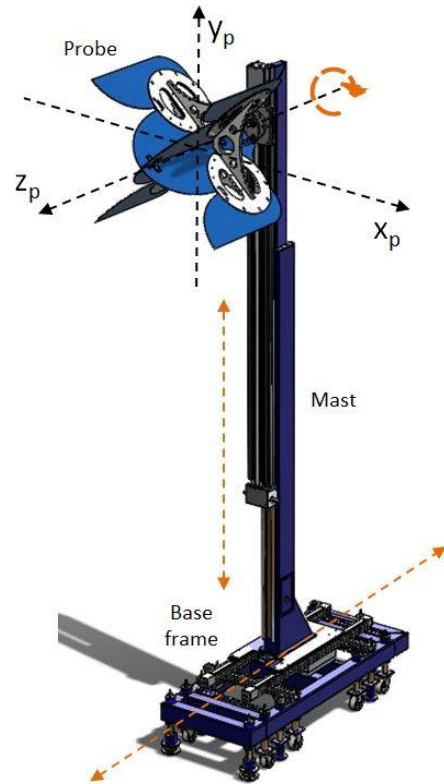


Figure 3. Overview of the updated probe positioner

#### A. Positioning repeatability and attitude control

As mentioned herein before, the probe positioner is equipped with three pistons, such as depicted in Figure 4.

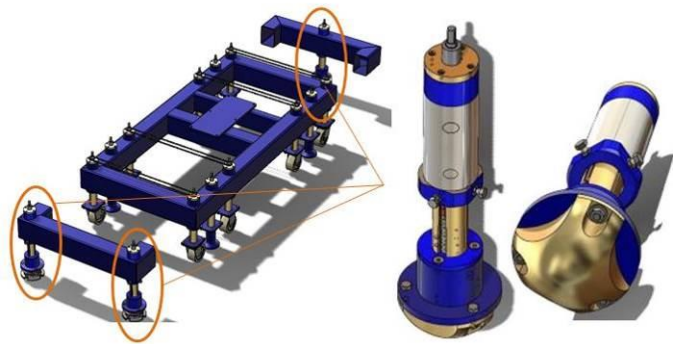


Figure 4. Details of the piston with anchor hemispheres

Every piston mainly consists of:

- A spherical part, that acts like a ball joint, once this is settled into a steel spherical container, provided for this



purpose and permanently clamped to the chamber's floor (see Figure 5.)

- A cylindrical slider, that allows a user to make vertically move the spherical part within the piston's body, by simply acting onto a removable crank (which drives a screw-nut connection)
- A cylindrical body, that enables the piston to be clamped onto the structural frame of the positioner.

This tripod of pistons enforces an identical positioning at each use, since every spherical part of a piston has to be combined to its dedicated ground-container. Of course, such a link provides the desired repeatability, by assuming that both the mechanical stiffness of the positioner's frame and the stiffness of each piston be high enough.

Moreover, each connection piston + ground-container forms a ball joint connection. On the whole, the three "spherical joint" connections grant to the positioner an overall "ball joint" degree of freedom. Consequently, this particularity enables the user to adjust the pitch and roll attitude of the positioner, by slightly acting onto each piston. As a result, any AUT placed at the end of the positioner's mast can be aligned into the required pointing direction.



Figure 5. Integrated piston with anchor hemisphere and dedicated spherical container on the chamber floor

### B. Ergonomy

The choice of extending the stroke of the Y-sliding axis was made to improve ergonomic aspect. Indeed, as shown in Figure 6. it is possible to drop the probe down to human height. This allows the operator to work on the probe without moving the base frame or using elevation device and inherent absorbers pulling. This feature allows then to save time once the probe positioner is installed. Figure 7. shows the expanded configuration when the probe is settled and aligned with the AUT coordinate system.

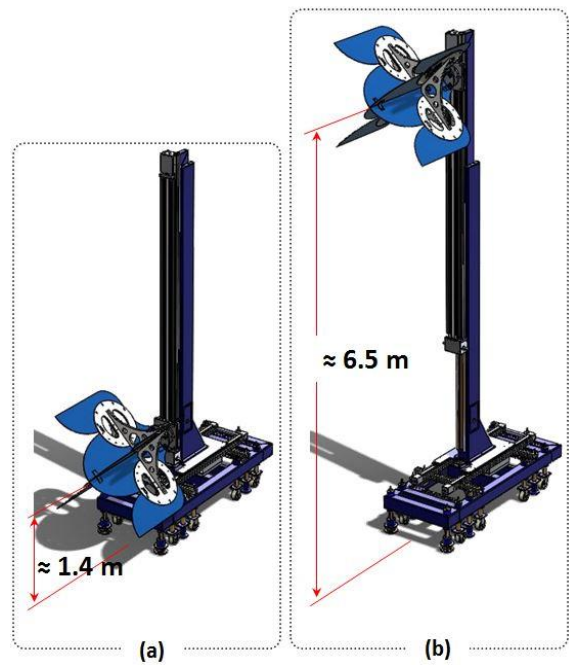


Figure 6. Views of the extreme y-location of the probe  
(a) compressed configuration  
(b) expanded configuration



Figure 7. Photograph of the measurement probe in the measurement (expanded) configuration

### IV. OPTICAL ALIGNMENT TOOL

The optical alignment tool shown in Figure 8. has been developed to align the measurement probe with the AUT spherical coordinate system. As this last is well known and trusted thanks to the positioner accuracy the alignment tool is located in place of the AUT and looks toward the measurement

probe. The tool is composed by a laser telemeter providing the measurement distance and by an ethernet camera providing an image in front of the probe.

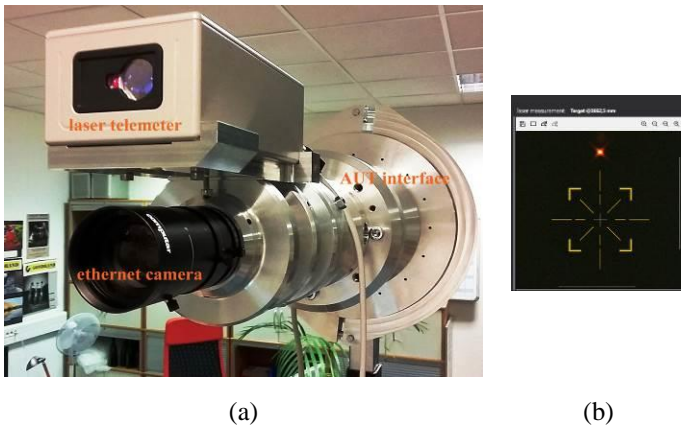


Figure 8. (a) Photograph of the optical alignment tool  
(b) Screenshot of the viewport

The mechanical flange has been designed in such a way to ensure perfect alignment with the positioner interface by mounting the instruments. Then instruments have been calibrated with a reference image target. A specific user interface has been developed to allows the operator to optically appreciate the good alignment of the probe with the reference target (cf. Figure 8. b). By setting  $\varphi = 0^\circ$  and  $\theta = 0^\circ$ , the probe is settling in the right location and orientation thanks to the adjusting axes presented before.

## V. REFERENCE ANTENNA

Reference antenna is a difficult point when low frequencies are considering. Indeed the lack of measurement facility with mastered uncertainties as well as the mechanical robustness – due to large dimensions – implies a very few number of reference antenna from which can be estimated the AUT gain. Herein we propose to design, realize and test a wide band reference antenna dedicated to our system. The measurement goal is twice. First we need an antenna providing good linear polarization to calibrate the measurement probe. Secondly we need a reference gain or efficiency. The first one implies planar antenna with very low mechanical deformation when performing the roll scan in front of the probe during the calibration process. Moreover an emphasis was placed on the ease to use of this antenna in term of mass and covered bandwidth. The second one implies to well know the performances of the antenna and its stability over time. As it is difficult to know her with trust through measurement results, the choice was made to design the antenna fully or mainly metallic and exploit performances coming from simulation. The following paragraphs present briefly the mechanical and electrical properties of the manufactured reference antenna. Some radiation pattern measurement results are provided to appreciate the polarization quality.

### A. Mechanical properties

As shown in Figure 9, the topology of this antenna is based on the existing measurement probe (dual Vivaldi). All the antenna body is made with aluminum to save mass. The outline is realized with arched T-shape profiles and planes are filled with aluminum lattice. To ensure mechanical strength during the roll scan two reinforcement structures are present on the antenna basament and small pieces of polyacetal in the slots. The resulting antenna is globally mainly planar and fully planar on the radiating part (30 mm thick). Overall dimensions are 3 m long by 1.95 m height and the global mass is 50 kg. Considering the covered bandwidth (40 – 400 MHz) the antenna could be considered quite compact.

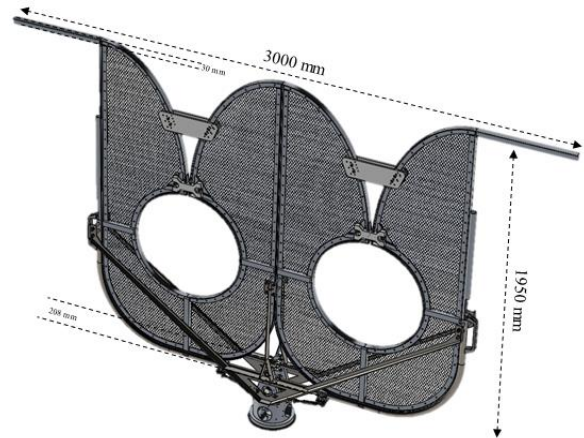


Figure 9. Mechanical model of the reference antenna

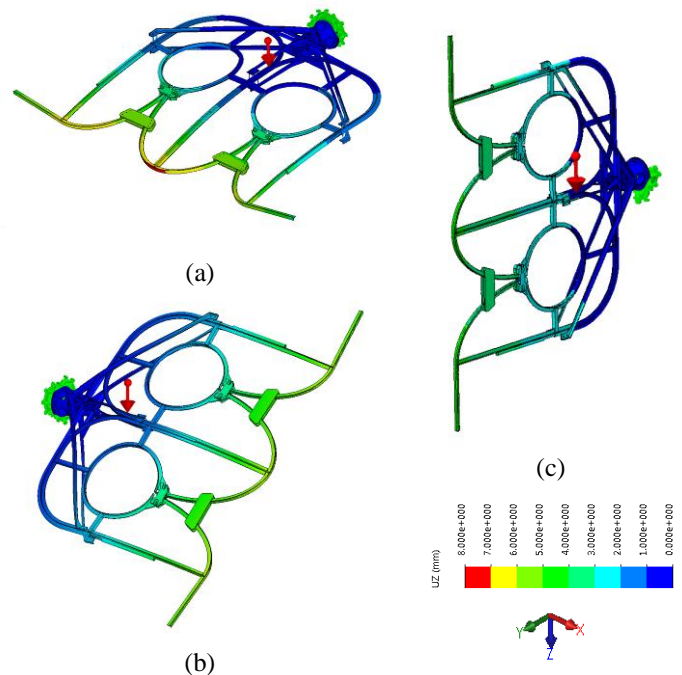


Figure 10. Simulated mechanical displacement under dead load only - (a) H, (b) 45° and (c) V configuration - Magnified display (deformed scale = 42:1)



Specific mechanical simulations were performed to check the deformation due to the antenna's dead load for three orientations namely horizontal, vertical and 45°. The worst case is the horizontal orientation with a maximum displacement of 8 mm on the antenna top as shown in Figure 10. This displacement is acceptable regarding the large dimensions and the large wavelengths. Figure 11. presents the manufactured antenna during the validation measurements.



Figure 11. Photograph of the reference antenna during validation measurements

### B. Electrical properties

The manufactured reference antenna has been characterized in terms of return loss and radiation pattern for different orientations. Figure 12. presents the simulated and measured (outdoor) return loss for the three orientations as considered in the mechanical study. We obtain a good stability versus the orientation and quite good agreement with simulation results considering a return loss better than -8 dB from 40 MHz to 400 MHz.

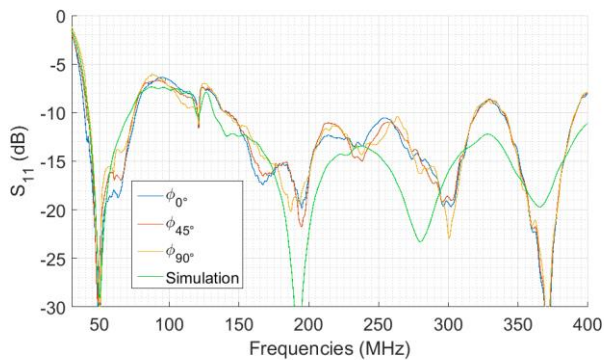


Figure 12. Measured and simulated return loss for different orientations of the reference antenna

Concerning the radiation results, Figure 13. shows boresight directivity obtained through simulation and measurement. Differences can be obtained in terms of frequency shift and absolute level, but results are acceptable with a minimum of 1.4 dBi and a maximum of 8.8 dBi on the whole frequency band. Figure 14. Figure 15. and Figure 16. compare simulated and

measured radiation patterns of the two main cuts for 60 MHz, 110 MHz and 200 MHz respectively. Obtained results are conclusive and the boresight cross polarization level remains lower than -30 dB.

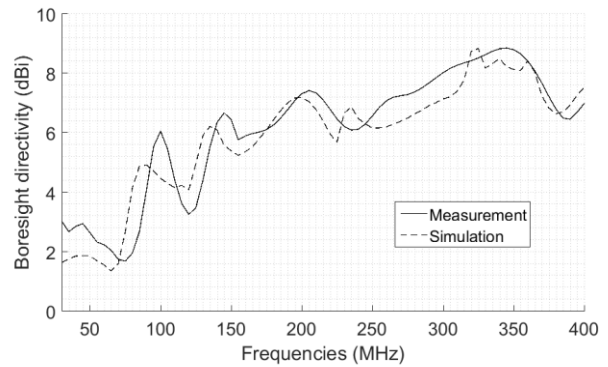


Figure 13. Measured and simulated boresight directivity

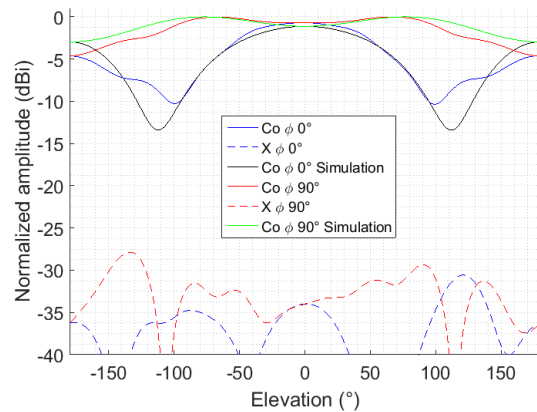


Figure 14. Measured and simulated radiation pattern at 60 MHz

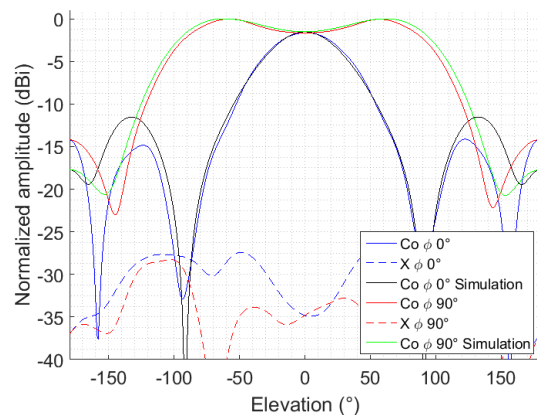


Figure 15. Measured and simulated radiation pattern at 110 MHz

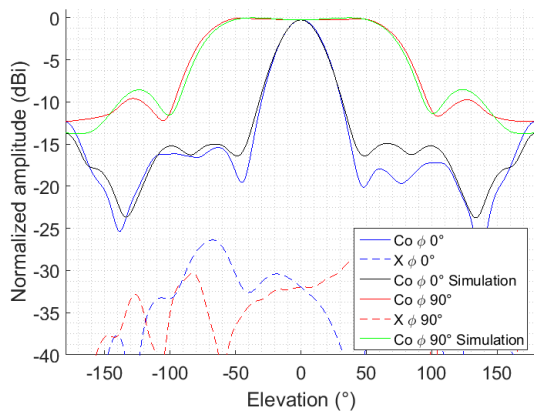


Figure 16. Measured and simulated radiation pattern at 200 MHz

## VI. POST-PROCESSING TOOL

To complete this near-field measurement system, a specific user interface has been developed and a snapshot is shown Figure 17. This interface allows the operator to perform all the post-processing steps to obtain far-field results from near-field measurement data. Steps are mainly the following: apply calibration coefficients – define and apply a time windowing – perform the near-field to far-field transformation and save

results in a dedicated format. All steps are accompanied by visualization control for the full sphere data.

## VII. CONCLUSION

In this paper was presented the complete implementation of a single probe near-field system installed in the CATR CNES chamber. The full system has been defined, each part has been described and validated through mechanical and electrical simulations and/or measurements. Intensive studies during last years allow to obtain a system comprising hardware updates and creations (including positioning repeatability and ergonomic aspects), specific reference antenna and a post-processing tool. All these development aim to know, reduce and master the measurement results uncertainties. These last have been recently estimated during a specific measurement campaign. Results will be presented in a future communication.

## REFERENCES

- [1] G. Le Fur et al.; "Uncertainty Analysis of Spherical Near Field Antenna Measurement System at VHF", in 36th AMTA Annual Meeting & Symposium, Tucson, Az, USA, October 2014.
- [2] G. Le Fur et al., "Comparison of antenna measurement results in disturbed environment using a VHF spherical near field system," Antenna Measurements & Applications (CAMA), 2014 IEEE Conference on, Antibes Juan-les-Pins, 2014, pp. 1-4
- [3] G.E. Hindman and A.C. Newell, "Spherical near-field self-comparison measurements," in 26th AMTA Annual Meeting & Symposium, Atlanta, Ga, USA, October 2004

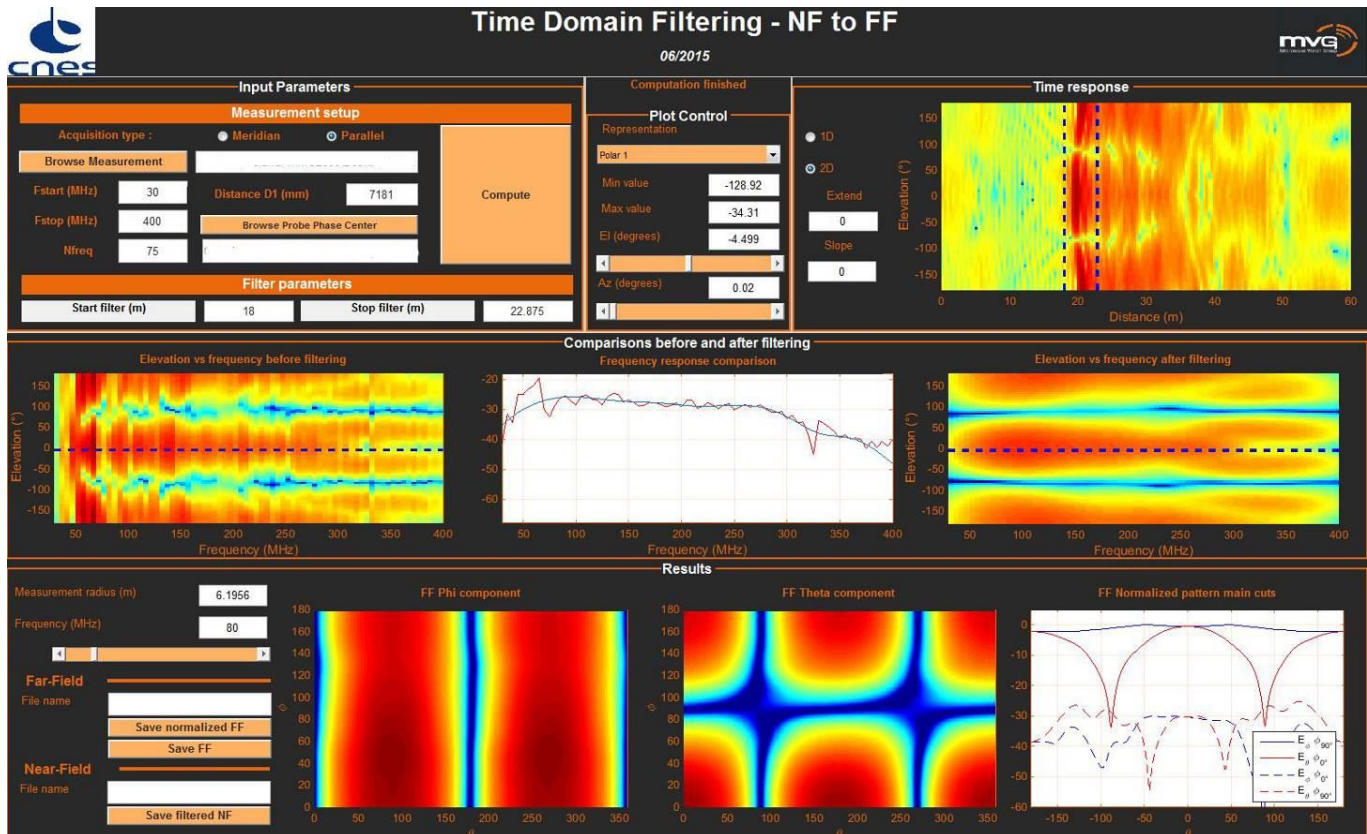


Figure 17. Snapshot of the post-processing tool

